Walk the Walk

A Lightweight Active Transtibial Prosthesis

IMAGE LICENSED BY GRAPHIC STOCK

By Qining Wang, Kebin Yuan, Jinying Zhu, and Long Wang

Active transtibial prostheses that can overcome the deficiencies of passive prostheses are gaining popularity in the research field. In addition to the advantages in joint torque and gait symmetry, terrain adaptation and total weight are other benefits that can help push active prostheses into the commercial market. In this article, we present a lightweight robotic transtibial prosthesis with damping behaviors for terrain adaptation. The proposed prosthesis, which mainly consists of a low-power motor, weighs only 1.3 kg, excluding the battery. It focuses on terrain adaptation instead of providing positive work at the stance phase. A damping control strategy is proposed to enable the prosthesis to manipulate the ankle impedance during stance with little power consumption. Experiments with three amputee subjects using the robotic prosthesis on different terrains show similar angle trajectories to the intact limb during the controlled flexion (CF) period as well as improved gait symmetry and walking stability compared with the robotic prosthesis in the maximal damping mode. The average power consumption of the prosthesis during one gait cycle is around 3.5 W, and a 0.28-kg rechargeable lithium-ion (Li-ion) battery can sustain a usage duration of more than 12 h or 20,000 steps.

Digital Object Identifier 10.1109/MRA.2015.2408791
Date of publication: 26 August 2015

Existing Transtibial Prosthesis Technology

A recent national statistics report says there are over 2 million upper- and lower-extremity amputees in China [1]. Most lower-limb amputations are commonly transtibial or

1070-9932/15©2015IEEE

transfemoral. The main way to regenerate a bipedal gait for a walking amputee is by using a lower-extremity prosthesis [2]. Most existing commercial transtibial prostheses are energetically passive without actuation. Although these prostheses have improved the quality of amputees' lives, they have several deficiencies. Amputees using these passive prostheses exhibit asymmetrical gait patterns [3]. In addition, without providing net positive work, passive prostheses require amputees to consume 20–30% more metabolic energy to walk at the same speed as able-bodied individuals [4].

To deal with these limitations, increasing efforts have been made to improve active transtibial prostheses during the last few decades, e.g., [5]–[11]. According to the joint actuation types, existing active transtibial prostheses can be roughly divided into two main categories. The first is the pneumatic actuator-based transtibial prosthesis. In 1998, Klute et al. [6] built a transtibial prosthesis powered by an artificial pneumatic muscle (the Mckibben actuator). Versluys et al. [7] designed another prosthesis powered by pneumatic cylinders. Although these pneumatic actuators are capable of providing enough force to propel amputees, their control difficulties, low position accuracy, and large size, due to the high-pressure air pump have restrained the development of pneumatic prostheses.

The second category is the motor-driven prosthesis. Au et al. [5] developed a powered ankle-foot prosthesis that can reduce the amputee's metabolic consumption by 14% on average. The prosthesis uses a combination of a spring and a motor-driven series elastic actuator (a 150-W brushless Maxon dc motor). A unidirectional spring structure placed parallel to the ankle joint makes the ankle stiffer during dorsiflexion than during plantar flexion. Another important example is the SPARKy prosthesis which uses a motor-driven robotic tendon actuator (150-W dc motor) [8]. Commercial versions of the two prostheses have been released by BiOM [12] and Spring Active [13], respectively. Recently, Cherelle et al. [10] proposed a new concept for an energy efficient transtibial prosthesis, which uses a low-power actuator that stores energy in the springs during the early and middle stance phase and releases the energy during the push-off phase.

Though these motor-spring mechanism-based transtibial prostheses do improve the energy efficiency of amputees, the prostheses are limited by their weight. Focusing on providing sufficient positive work and a longer operating duration, these prostheses are usually composed of a parallel spring, a high-power motor, and a large-capacity battery. Consequently, the weight of an active prosthesis can be more than 2 kg [10]–[12]. A heavy prosthesis tends to increase the knee extension load and cause larger interaction force between the adaptor and the residual limb. Furthermore, in addition to the inability to provide assistive torque, the inability of a passive prosthesis to adapt to terrain variations leads to gait asymmetry and walking instability [14], [15]. Ossur's Proprio Foot [16] is a typical commercial attempt at terrain adaptation. This is done without providing assistive torque beyond the energy that is stored during dorsiflexion and then returned prior to toe-off. But it can only adjust the ankle angle to prepare for the next stance phase during swing without adjusting the ankle impedance during the stance phase.

Focusing on terrain adaptation instead of providing high joint torque, we present the design and control of a lightweight robotic transtibial prosthesis. A novel damping control strategy based on the motor-winding short is proposed to enable the prosthesis to manipulate the ankle impedance during stance with little power consumption. Three amputee subjects were recruited to perform walking experiments on different terrains, including level ground (LG), stairs (ascending and descending), and ramps (ascending and descending). Experimental results with the robotic prosthesis show improved ankle angle trajectories, gait symmetry, and walking stability of amputee subjects.

Robotic Transtibial Prosthesis Prototype

Instead of using high-power motors to obtain large joint torque, we designed a lightweight motor-driven robotic transtibial prosthesis for terrain adaptation, the Peking University Robotic Transtibial Prosthesis (PKU-RoboTPro).

The prototype of the proposed prosthesis is shown in Figure 1(a). The current version is an integrated one that uses all the modules in the transtibial prosthesis including mechanical structure, control circuits, sensors, and battery. The model of the ankle joint can be simplified as a three-bar mechanism, which comprises bars *a*, *b*, and *c*, and three hinges, *A*, *B*, and *C*, as shown in Figure 1(b). To visualize the model, *a* can be seen as the foot, *b* as the shank, and *C* as the ankle joint. Made up of a motor-driven ball screw transmission, *c* is a customized bar. The screw pitch is 2 mm. The motor system uses a 50-W dc brushless motor from Maxon (EC 45 50 W), equipped with a 5.8:1 reduction gearbox. The angle range of the ankle joint is from 25° dorsiflexion to 25° plantar flexion. The total weight of the proposed prosthesis (excluding the rechargeable Li-ion battery) is 1.3 kg.

A damping control strategy is proposed to enable the prosthesis to manipulate the ankle impedance during stance with little power consumption.

Three kinds of sensors are installed on the prosthesis, including one load cell, one angle sensor, and two inertial measurement units (IMUs), as shown in Figure 1(a). The single-axis load cell [Model LBS (Load Button Small) Miniature Compression Load Button] has a measurement range of 0–250 lbf and is used to detect the interaction force between the residual limb of the amputee and the prosthesis. The absolute angle sensor (Angtron-RE-25) is used to measure the ankle angle with a 0–360° range and 12-b resolution. The two IMUs are used to measure the inclination angle and other inertial information such as

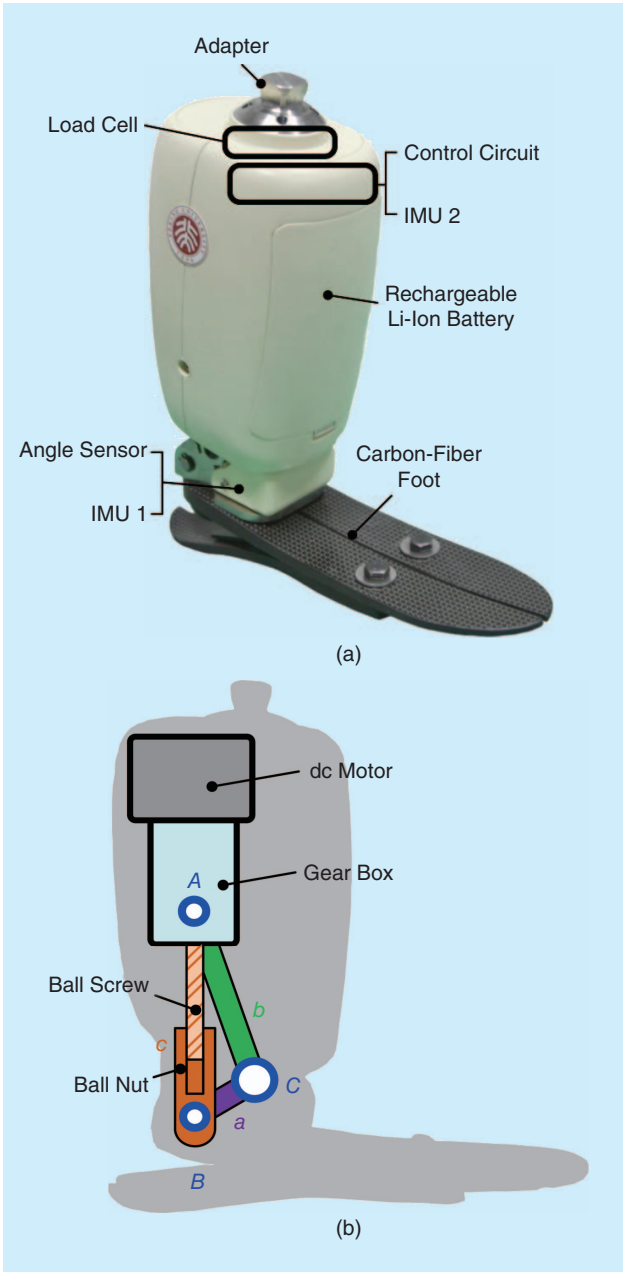

Figure 1. (a) The prototype of the proposed prosthesis (PKU-RoboTPro), including an active ankle joint and a carbon-fiber foot. All of the modules, including the mechanical structure, control circuits, sensors, and battery have been integrated in the prosthesis. The installed sensors include one angle sensor, one load cell, and two IMUs (IMU 1 is placed on the foot, and IMU 2 is placed on the shank). The total weight of the prosthesis is 1.3 kg (excluding the rechargeable Li-ion battery), which is comparable to the able-bodied limb. (b) The ankle model, simplified as a three-bar mechanism comprising three bars, *a*, *b*, and *c*, and three hinges, *A*, *B*, and *C*, where *a* can be seen as the foot, *b* as the shank, and *C* as the ankle joint.

the acceleration and the rotation rates. One IMU is installed on the upper surface of the foot, and the other is installed on the shank of the prosthesis. Each IMU has an embedded triaxis gyroscope and a triaxis accelerometer. The gyroscope has a full-scale range of 2,000°/s and a resolution of 0.06°/s, while the accelerometer has a full-scale range of 157 ms^2 and a resolution of 0.005 ms^2.

Motor-Driven Nonlinear Damping

The main subdivisions of one gait cycle are the stance phase, when the foot is on the ground, and the swing phase, when the foot is off the ground. The stance phase of LG walking can be further divided into three subphases: controlled plantar flexion (CP), controlled dorsiflexion (CD), and powered plantar flexion (PP) [17]. Together, CP and CD make up the CF phase. The human ankle provides different functions during different phases of one gait cycle [18]. During CF, the ankle absorbs the foot-strike shock, stores the kinetic energy of walking, and enables the body's center of gravity to move forward smoothly. During PP, the ankle provides net positive work to propel the body upward and forward, and during swing, the ankle behaves as a position source to achieve foot clearance and reset the ankle to the equilibrium position. As for adaptation to terrain variations, the vital phase is the swing phase as well as the CF phase. During swing, the ankle joint adjusts to an appropriate angle to get prepared for the foot strike on the new terrain. During CF, the ankle behaves as a spring (or a spring and a damper) and provides resistive torque to prevent the ankle joint from plantar flexing or dorsiflexing too quickly. As for the robotic prosthesis in this article, the proposed control method does not focus on assistive torque during PP but concentrates on the ankle behavior of providing resistive torque during CF, which can be another important issue that influences the amputee's walking behaviors and his/her acceptance of wearing a robotic prosthesis.

Kinetics of Intact Ankle During CF

According to the rotation kinetics, the ankle motion during the CF phase can be described by

$$\tau_m - \tau_a = I\ddot{\theta}, \tag{1}$$

where τ_m refers to the motive torque that drives the joint to rotate, τ_a refers to the resistive torque provided by the ankle joint that prevents the joint from rotating, and I refers to the rotational inertia of the shank. According to the spring-damper model, the ankle torque τ_a can be modeled as

$$\tau_a = k(\theta - \theta_e) + b\dot{\theta}, \tag{2}$$

where k, b, and θ_e denote the linear stiffness, damping coefficient, and equilibrium ankle angle, respectively, and these coefficients vary with different gait phases [19]. To mimic the resistive torque of the ankle with the motor-driven prosthesis, we proposed a novel damping control method. This method does not need auxiliary components such as springs and dampers, and it consumes little electrical power.

Implementation of Damping Control

During bipedal locomotion, the center of mass (CoM) of the human body moves forward, and the movement of CoM

results in the rotation torque τ_m during the CF phase. τ_m drives the ankle joint to plantar flex during the early stance and dorsiflex during the middle stance, resulting in the motor rotation. A motor can behave as a generator when the motor rotates, and the rotation will generate an induced voltage E_a,

$$E_a = C_E \phi n, \tag{3}$$

where C_E refers to the electromotive constant, ϕ refers to the magnetic field intensity, and n refers to the motor speed.

If the stator windings of the brushless motor (or rotor windings of the brushed motor) are shorted, the induced voltage will generate a current I_a, and its instantaneous value can be estimated by

$$I_a = \frac{E_a}{R_a}, \tag{4}$$

where R_a refers to the motor armature resistance.

I_a will produce a braking torque τ_b that prevents the motor from rotating

$$\tau_b = C_T \phi I_a = \frac{C_T C_E \phi^2}{R_a} n, \tag{5}$$

where C_T refers to the motor torque constant.

According to (5), the braking torque τ_b is proportional to the motor speed n. As the motor armature resistance R_a is usually very small (0.98 Ω for our motor), the resulting braking torque τ_b will be quite large once the motor rotates.

If we switch the motor-winding-short on or off with a pulsewidth modulation (PWM) signal, the braking torque during the switch-on period will be very large and the ankle joint will only be able rotate at a low speed, while the braking torque during the switch-off period will be small and the joint will be able to rotate quickly. With an appropriate on/off frequency, the braking torque will be positively correlated with the duty cycle (D) of the PWM signal, and the resulting equivalent braking torque (τ_{eb}) can be approximated as

$$\tau_{eb} = k_d D n. \tag{6}$$

As the duty cycle D determines the relationship between the torque and the speed, it can be regarded as the damping coefficient. k_d is the proportionality coefficient in the unit of Nm/(r/min).

To verify the effectiveness of (6), the braking torque was evaluated under two experimental conditions.

- D is constant (50%), and n varies from 400 to 1,250 r/min.
- n is constant (600, 800, and 1,000 r/min, respectively), and D varies from 20 to 80%.

The evaluated motor, which acted as a generator during the experiment, was driven by another motor whose output shaft was connected in series with that of the evaluated motor. The braking torque was estimated by the average armature current, with the torque constant of 33.5 mNm/A provided by the motor data sheet.

A prosthesis in the maximal damping mode without control can only move within a limited angle range (less than 8°).

The evaluation results of the proposed method are shown in Figure 2. The braking torque is proportional to the motor speed at a constant PWM duty cycle D, as shown in Figure 2(a). The braking torque is proportional to the duty cycle D at a constant speed, as shown in Figure 2(a). These results verified that the braking torque resulted from the motor winding short can be effectively estimated by (6).

The implementation process of the proposed damping control onto the prosthesis prototype is shown in Figure 3. The human bipedal locomotion generates a driving torque,

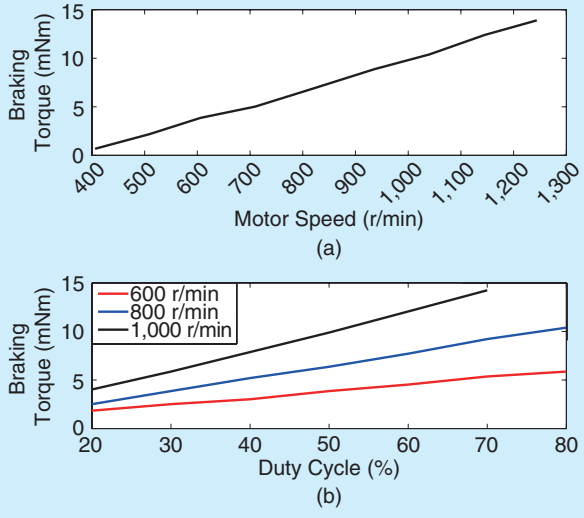

Figure 2. An evaluation of the proposed method for braking torque control under two different conditions: (a) the motor speed and (b) the duty cycle.

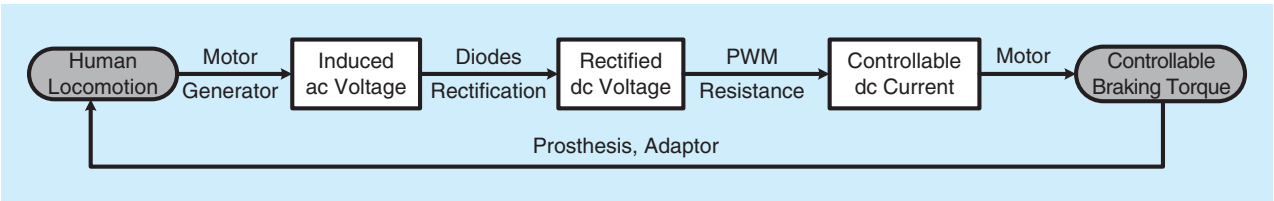

Figure 3. The realization process of the proposed braking torque control on the prosthesis prototype.

and the torque drives the motor to rotate. The rotating motor produces the induced voltage as a generator. Note that the induced voltage is alternating as its direction varies with different motor phases, and the ac voltage cannot be controlled directly until it is rectified to the dc voltage by a full-bridge rectifier made of six diodes. With the controlled short on/off by the PWM signal, the dc voltage is transferred to the controlled dc current, and the PWM acts as a variable resistance. After that, the dc current produces the braking torque to prevent the motor from rotating, which then affects the human locomotion.

Kinetics of Prosthetic Ankle During CF

As for the proposed robotic prosthesis, the ankle torque can be described by

$$\tau_a = k_T \tau_{\text{eb}} + \tau_f, \tag{7}$$

where k_T refers to the transmission ratio between the motor output torque and the resulting ankle joint torque, τ_{eb} refers to the braking torque resulting from the motor winding short of (6), and τ_f refers to the friction torque caused by the mechanical transmission.

Substituting (7) into (1), the rotation kinetics of the ankle prosthesis during the CP and the CD phases could be described by

$$\tau_m - k_T \tau_{\text{eb}} - \tau_f = I\ddot{\theta}. \tag{8}$$

If the motor windings are not shorted and $\tau_{\text{eb}} = 0$, τ_m will drive the ankle joint to rotate quickly as the friction torque τ_f is much smaller than τ_m. On the contrary, if the motor windings are shorted, the braking torque τ_{eb} will be quite large and make the ankle rotate at a very low speed. In this way, the prosthesis motor uses the human kinetic energy during walking to produce the braking torque and does not consume electric energy during stance.

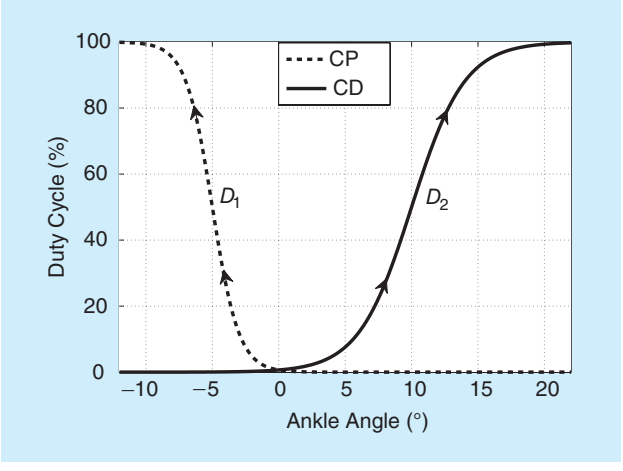

Figure 4. The damping control function of the CP and CD phases. $s_1 = 0.25$, $s_2 = 0.5$, $\theta_{d1} = -5$, and $\theta_{d_2} = 10$. The controller switches between these two functions according to the angular rate.

Gait Control for Different Terrains

The locomotion kinematics and kinetics of the ankle joint on LG are quite different from the kinematics and kinetics on stairs and ramps [20], [21]. Note that since we do not focus on providing a large assistive torque during the late stance, the gait phase divisions can be uniformly simplified into the CF phase and the swing phase. The ankle locomotion variation on different terrains can be summarized as different ankle impedance (torque-angle relationship) during CF and different ankle equilibrium angles during swing. The proposed prosthesis performs damping control for the CF phase and position control for the swing phase. The transition between the CF and swing is detected by the load cell with a simple threshold method.

Damping Control for CF

According to (6), the ankle impedance during CF is simplified as the damping coefficient D, and the control strategy becomes designing the damping-angle relationship. At the early stance, the ankle resistive torque is expected to be small to enable shock absorption and keep the foot flat. At the middle stance, the driving torque τ_m increases as the CoM moves forward, and the ankle torque is expected to increase to prevent the ankle from dorsiflexing too fast. When the ankle reaches the maximal dorsiflexion, the ankle resistive torque is expected to be large enough to prevent the ankle from rotating. For preliminary implementation, the damping-angle relationship is designed as a hyperbolic tangent function.

As shown in Figure 4, the controller switches between the damping function of the CP (D_1) and the damping function of the CD (D_2) according to the angular rate $\dot{\theta}$,

$$\begin{aligned} D &= \begin{cases} D_1, & \dot{\theta} < 0 \\ D_2, & \dot{\theta} \geq 0 \end{cases} \\ D_1 &= 1 - 0.5(\tan h(s_1(\theta - \theta_{d1})) + 1) \\ D2 &= 0.5(\tan h(s_2(\theta - \theta_{d2})) + 1), \end{aligned} \tag{9}$$

where θ_{d1} is the threshold plantar flexion angle, θ is the current joint angle, s_1 is the sensitivity factor that decides the slope of the function, and the resulting D_1 is the duty cycle of the PWM signal that controls the motor terminal short. The threshold dorsiflexion angle is θ_{d2}.

Position Control in Swing Phase

As for the swing phase, a proportional-derivative (PD) position controller is proposed,

Table 1. The control parameters for different terrains.

	θ_0 (°)	θ_{d1} (°)	S_1	θ_{d2} (°)	S_2
LG	0	−5	0.5	10	0.25
Stair Ascent (SA)	6	—	—	12	0.4
Stair Descent (SD)	−5	−10	0.2	20	0.3
Ramp Ascent (RA)	12	10	0.5	15	0.5
Ramp Descent (RD)	3	−5	0.4	20	0.3

Table 2. Detailed information of the amputee subjects.

Subject	Age	Weight (kg)	Height (cm)	Gender	Amputation Leg	Years Postamputation	Prosthesis
Amputee 1	46	70	170	Male	Left	8	Otto bock 1S90
Amputee 2	26	73	174	Male	Right	5	Teh lin BK6060
Amputee 3	28	68	169	Male	Left	6	Otto bock 1C60

$$D = k_p(\theta_0 - \theta) + k_d(\dot{\theta}_0 - \dot{\theta}), \tag{10}$$

where D is the controller output for the motor driver, k_p and k_d are predefined constants, and θ_0 and $\dot{\theta}_0$ are the desired equilibrium angle and desired angle velocity of swing, respectively.

The five control parameters for different terrains are shown in Table 1. The symbol "—" means that the parameter for this terrain is not used, as there is no CP phase during stair ascent (SA).

Experimental Methods

Three unilateral transtibial amputee subjects participated in the experiments to verify the effectiveness of the designed prosthesis and the proposed control method. Detailed information on each of the amputee subjects is shown in Table 2. The amputee participants were experienced at prosthesis ambulation. All participants provided written, informed consent prior to participation.

The experiments consisted of a training session and a test session. During the training session, the five parameters in Table 1 were tuned according to the amputees' comfort feedback and enabled them to move on different terrains with symmetric gait patterns. During the test session, the subjects were required to perform LG walking, SA, stair descent (SD), ramp ascent (RA), and ramp descent (RD) with the robotic prosthesis. Terrain transitions between LG and the other terrains were managed by the operator with a wireless transmitter. The proposed prosthesis was first set to the maximal-damping mode without control to simulate the passive prosthesis as the subjects' commercial prostheses are quite different. In the maximal-damping mode, the robotic prosthesis presents a fixed impedance as the passive prostheses, and the ankle joint can only move slowly within a small angle range. Then, the prosthesis was set to the proposed damping control mode and repeated the same locomotion. In each mode, locomotion on five terrains was repeated ten times. The stair terrain consisted of four stairs. Each stair was 0.75 m in width, 0.40 m in depth, and 0.14 m in height. The length of the ramp terrain was 2.20 m, and the ramp inclination angle was 13.7°.

Three kinds of sensors are installed on the prosthesis, including one load cell, one angle sensor, and two inertial measurement units.

During each trial, the ankle angle trajectory of the prosthetic side and the ground reaction force (GRF) of both sides were measured. The angle was first measured by the onboard angle

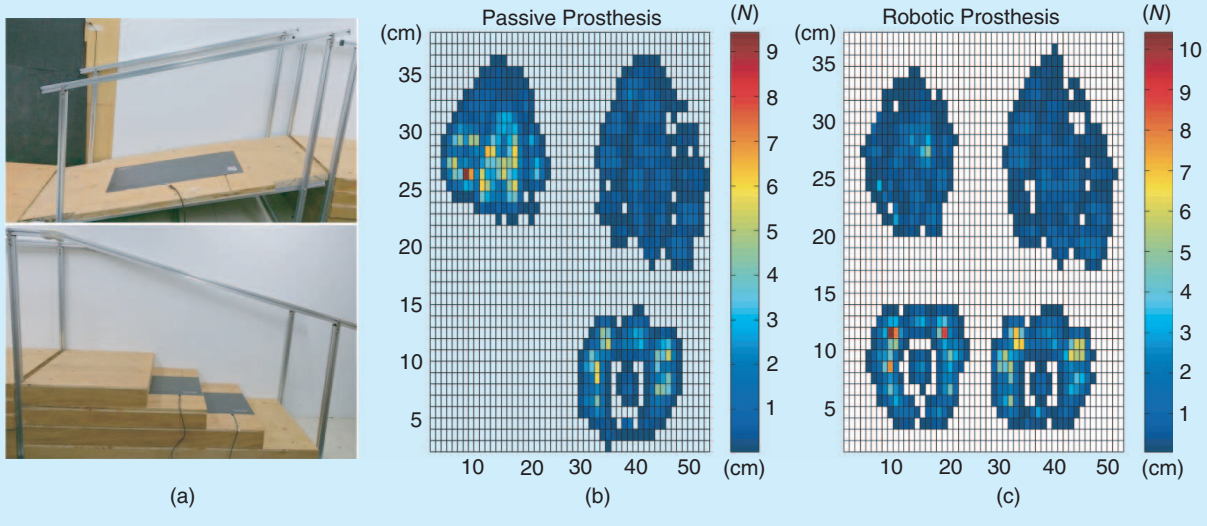

Figure 5. The experimental terrains with embedded force plates and the GRF measurement results of prostheses in different control modes: (a) The stair and ramp terrain with embedded force plates, (b) the GRF measurement results with the robotic prosthesis in maximal damping mode during RA, and (c) the GRF measurement results with the robotic prosthesis in damping control mode during RA. The color depth depicts the amplitude of GRF.

sensor in the prosthesis, and then sent to the PC by the wireless transmitter (nRF24L01). The sampling rate was 100 Hz, and the sampled data were low-pass filtered by a third-order Butterworth filter with a cutoff frequency of 10 Hz. Both the power data and the angle data were normalized to one gait cycle. To measure the GRF of both sides, two force plates [foot scan two-dimensional (2-D) 0.5-m plates, produced by RSscan International] were embedded into the second and third stair, one force plate (footscan 2-D 1-m plate) was embedded into the middle of the ramp, as shown in Figure 5. Another force plate (footscan 2-D 2-m plate) was put on LG to measure the GRF during LG walking. All the GRF data were sampled with a rate of 300 Hz.

To testify to the improvements of the proposed method, four indicators related to the gait symmetry and walking stability were calculated based on the GRF measurements [22].

- *Center of pressure (CoP) shift in medial/lateral (ML)*: In able-bodied gait, the medial/lateral CoP trajectory begins at the medial heel, moves laterally, and ends at the medial forefoot. Too much lateral excursion of the CoP trajectory is associated with increased instability [23].
- *CoP shift in anterior/posterior (AP)*: During locomotion on different terrains, the human ankle rotates to enable the body's center of gravity to move smoothly from the posterior heel to the anterior forefoot. The prosthetic ankle may result in a shorter CoP shift in AP because of its inability to rotate.

Table 3. Stride time on different terrains with and without damping control.

Stride Time (s)	Without	With
LG	1.33 ± 0.11	1.26 ± 0.03
SA	1.31 ± 0.09	1.30 ± 0.06
SD	1.28 ± 0.05	1.35 ± 0.07
RA	1.22 ± 0.03	1.21 ± 0.04
RD	1.23 ± 0.03	1.21 ± 0.06

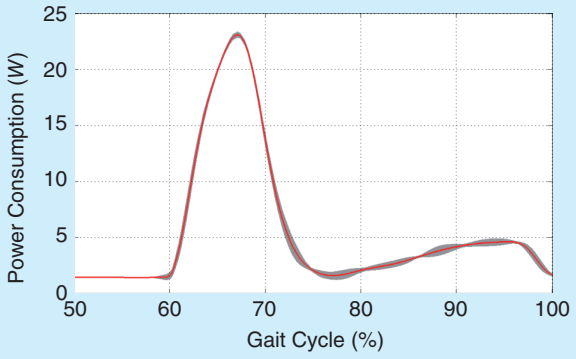

Figure 6. The power consumption of the robotic prosthesis during one gait cycle. The gray shaded area represents the standard error of mean.

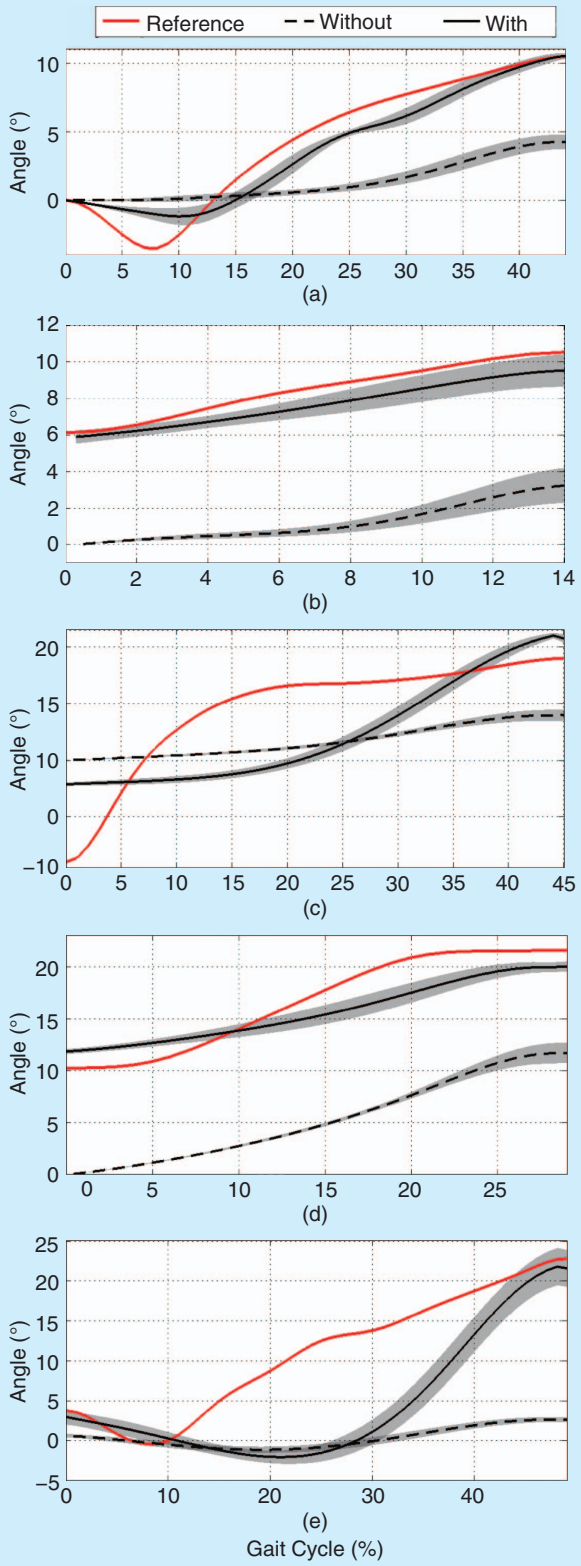

Figure 7. The ankle angle trajectories on different terrains: (a) LG, (b) SA, (c) SD, (d) RA, and (e) RD. The red line refers to the reference angle trajectory of the intact limb, the dashed black line refers to the angle trajectory of the robotic prosthesis in maximal damping mode without control, and the solid black line refers to the angle trajectory of the robotic prosthesis with damping control. The gray shaded area depicts the standard error of mean.

- *Normalized stance time*: Stance time refers to the period when the foot is on the ground, and the stance time of both feet is expected to be equal. As the walking speeds of different trials vary, the stance time of the prosthetic foot is normalized by that of the intact foot of the same trial.
- *Normalized peak GRF*: Peak GRF refers to the maximal GRF during stance. It is associated with a large impact on the residual limb and may lead to unstable or asymmetric gaits. To evaluate the effect of the proposed control method, the peak GRF measured in the damping control mode (robotic) is normalized by that measured in the maximal damping mode (passive).

The power consumption during one gait cycle was also measured to evaluate the duration of the onboard battery. The current is sampled by the onboard current sensor with a sampling rate of 200 Hz. The raw current sensor was low-pass filtered by a third-order Butterworth filter with a cutoff frequency of 20 Hz.

Experimental Results

By wearing the PKU-RoboTPro, the amputee subject can perform natural walking gaits on different terrains in outdoor and indoor environments (please see the video file in IEEE *Xplore*). The terrain transition command was sent by the operator through a wireless transmitter one step before the transition takes place. The stride time of the amputees on different terrains with and without damping control are shown in Table 3. With damping control, the locomotion speeds of the amputees were increased on all terrains except for SD, which was because the prosthesis had a much larger angle range and the amputees became more cautious during SD. In addition to the stride time, three kinds of results were provided, the power consumption, ankle angle trajectories, and gait indicators.

Power Consumption

The power consumption curve during one gait cycle averaged over 30 steps for the three amputees during LG walking, as shown in Figure 6. The power consumption during the idle state is around 1.4 W. As the proposed damping control method uses human kinetic energy during walking to produce braking torque, the prosthesis does not consume any additional electric power except for idle power during stance. The main power consumption period is the swing phase when the prosthesis resets to the equilibrium position under position control, and the peak power is around 23.3 W. The average power consumption of normal walking during one gait cycle is around 3.5 W. With a 0.28-kg rechargeable Li-ion battery (energy density 195 W • h/kg, see www.lgchem.com), the prosthesis can be used for more than 12 h or 20,000 steps.

The average power consumption of the prosthesis during one gait cycle is around 3.5 W.

Ankle Angle Trajectories

The ankle angle trajectories on different terrains, averaged over 30 steps from three amputee subjects, are shown in

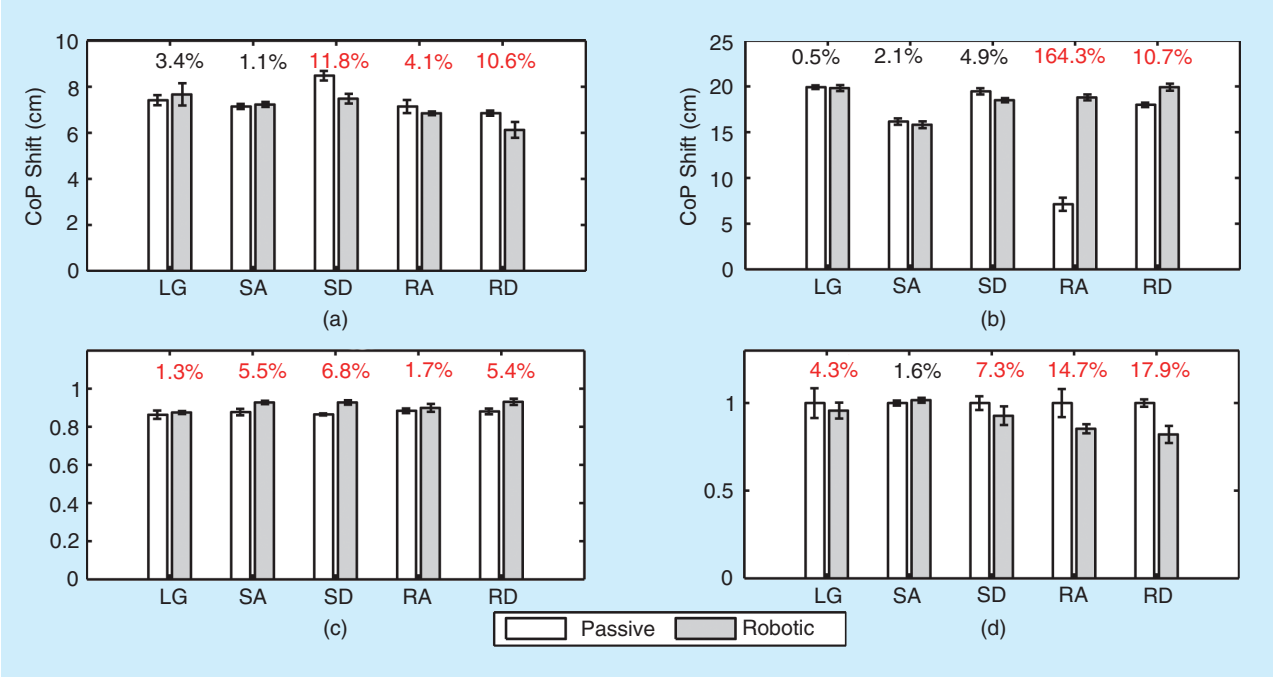

Figure 8. A comparison of different indicators between the passive and robotic prostheses: (a) CoP shift in ML, (b) CoP shift in AP, (c) normalized stance time, (d) normalized peak GRF. The experiments were carried out on LG, SA, SD, RA, and RD. The numbers above the bars express the variation quantity of the robotic prosthesis compared with the passive one. The red number means that the indicator has been improved, while the black number indicates performance deterioration.

Figure 7. The gait cycle starts with a heel strike, and only the CF portion of stance when the damping control works is shown. The reference angle data are from [20] and [21]. According to the figure, a prosthesis in the maximal damping mode without control can only move within a limited angle range (less than 8°). The ankle angle of the prosthesis without control starts with 0° for all the terrains, which is much different than an intact limb.

The braking torque was estimated by the average armature current, with the torque constant of 33.5 mNm/A provided by the motor data sheet.

The proposed robotic prosthesis has an angle range of ±25°, which is similar to that of the intact limb. With the proposed damping control strategy, the robotic prosthesis can adjust the ankle angle during swing and prepare for the new terrain of the next step. During stance, the damping of the ankle is adjusted according to the ankle angle, and the resulted angle trajectories can effectively mimic those of the intact limb, especially on terrains such as LG, SA, and RA. Angle trajectories during SD and RD are not quite similar to those of the intact limb. For the initial foot strike with the ground during SD, the amputees could not manage the toe strike with a plantar flexion angle as large as able-bodied individuals, so the initial angle of SD was set to be a smaller plantar flexion angle (6°). For RD, the CP was much slower than that of the intact limb, causing the trajectories to be quite different. This discrepancy was due to the fact that the amputees tended to be more careful when the prosthetic foot contacted the ground.

Gait Indicators

The calculated indicators of the proposed robotic prosthesis on different terrains are shown in Figure 8. The CoP shift in ML with the robotic prosthesis had a significant decrease from the passive one during SD and RD, while the indicator values on the other terrains did not change much. As for the CoP shift in AP, the robotic prosthesis had similar values to the passive one on LG and stairs, while the values on ramps had a significant increase, because the robotic prosthesis with damping control enabled full contact between the prosthetic foot and the ramp. Normalized stance time with the robotic prosthesis had greater values than that with the passive prosthesis, which indicated that the robotic prosthesis created a more symmetrical gait. As for the normalized peak GRF, values with different prostheses during SA did not vary a lot, while those with the robotic prosthesis were smaller than values with the passive prosthesis, especially during ramp ambulation. Smaller peak GRF implied a smaller impact on the residual limb. The four indicators show that the robotic prosthesis has improved the amputee's gait symmetry and walking stability.

Discussion

For the emphasis on terrain adaptation, instead of providing large assistive torque, the proposed robotic prosthesis with a low-power motor is quite lightweight. With the proposed damping control method, the prosthesis can manipulate the ankle impedance during stance and enable the amputee to smoothly move on different terrains. The amputee's gait symmetry and walking stability are improved, and the prosthesis with damping control has similar angle trajectories to the intact limb on LG and ascent terrains. The terrain adaptation ability of the prosthesis does improve the amputees' bipedal walking performance.

Compared with Ossur's Proprio Foot, which can only adjust the ankle angle during swing and lock the ankle during stance, allowing the carbon-fiber foot to store significant energy as it deflects in dorsiflexion and return it in plantar flexion [15], the PKU-RoboTPro employs a different strategy, trading the ability to store and return significant energy in a carbon-fiber spring for the capability of adjusting the ankle impedance during stance and adapting to different walking speeds and terrains.

Due to the lack of a parallel spring as well as a high-power motor, the PKU-RoboTPro cannot provide high assistive torque like the powered prostheses developed by BiOM [12] or SpringActive [13]. However, the lighter weight of the prosthesis can reduce the load of the residual limb and help the wearer to move more easily during the swing phase. In addition, the prosthesis consumes less energy during one gait cycle, which means the walking distance is farther for the same battery capacity.

Other reported active prostheses, e.g., the AMP-foot prosthesis, can output sufficient power during the late stance phase, but the ankle is not controllable during the early stance phase and the swing phase. Compared with AMP-foot, the PKU-RoboTPro can not only control the ankle damping during the stance phase but also adjust the ankle angle during the swing phase to bring foot clearance from the ground and prepare for the next stance phase.

The proposed robotic transtibial prosthesis PKU-RoboTPro, though promising, has its limitations and needs further improvements. The main limitation of the proposed prosthesis is that it can neither provide large assistive torque nor store significant energy in the carbon-fiber foot to return to the user. The peak torque of the prosthesis is around 50 Nm, which is not enough to walk fast. Further optimization for the balance between joint torque and prosthesis weight is needed. In addition, though the current system can perform smooth locomotion on different terrains with ankle damping behaviors, the damping control strategy needs to be improved to enable the prosthesis to mimic the intact limb more effectively. Further studies on integration of the locomotion mode recognition system and evaluation experiments on more distinguished terrain transitions may bring better gait behaviors.

Conclusions

In this article, we proposed a lightweight robotic transtibial prosthesis with damping behaviors for terrain adaptation.

Instead of focusing on providing large assistive torque, the proposed prosthesis mainly consists of a low-power motor and weighs only 1.3 kg, excluding the battery. A novel damping control strategy based on the motor-winding-short is proposed to enable the prosthesis to effectively mimic the ankle impedance during stance with little power consumption. Experiments involving three amputees with the robotic prosthesis on different terrains show similar ankle angle trajectories to the intact limb and improved gait symmetry and walking stability. The proposed prosthesis can be an important addition to the arsenal of active prostheses to help more transtibial amputees.

Future studies include mechanical structure optimization, ankle torque evaluation, and improvements of the control strategy on different terrains with the combination of locomotion mode recognition.

Acknowledgments

This article was supported by the 2011 R&D Project of the Beijing Disabled Persons' Federation, the National Natural Science Foundation of China (61005082, 61020106005), the Beijing Nova Program (Z141101001814001), and the 985 Project of Peking University (3J0865600). We would like to thank the anonymous reviewers for their valuable suggestions that improved this article. We would also like to thank Zhao and Mai for their contributions in circuit implementation.

References

[1] *China Disabled Persons Development Statistics Bulletin*, Chinese Disabled Persons' Federation, Beijing, China, 2012.

[2] M. Goldfarb, B. E. Lawson, and A. H. Shultz, "Realizing the promise of robotic leg prostheses," *Sci. Tranl. Med.*, vol. 5, no. 210, p. 210ps15, 2013.

[3] D. A. Winter and S. E. Sienko, "Biomechanics of below-knee amputee gait," *J. Biomech.*, vol. 21, no. 5, pp. 361–367, 1988.

[4] N. H. Molen, "Energy/speed relation of below-knee amputees walking on motor-driven treadmill," *Int. Z. Angew. Physiol.*, vol. 31, no. 3, pp. 173–185, 1973.

[5] S. K. Au, J. Weber, and H. Herr, "Powered ankle-foot prosthesis improves walking metabolic economy," *IEEE Trans. Robot.*, vol. 25, no. 1, pp. 51–66, Feb. 2009.

[6] G. K. Klute, J. Czerniecki, and B. Hannaford, "Development of powered prosthetic lower limb," in *Proc. 1st Nat. Meeting, Veterans Affairs Rehabil. R and D Service*, Washington, DC, 1998.

[7] R. Versluys, A. Desomer, G. Lenaerts, O. Pareit, B. Vanderborght, G. Perre, L. Peeraer, and D. Lefeber, "A biomechatronical transtibial prosthesis powered by pleated pneumatic artificial muscles," *Int. J. Model. Identif. Control*, vol. 4, no. 4, pp. 394–405, 2008.

[8] J. Hitt, T. Sugar, M. Holgate, R. Bellman, and K. Hollander, "Robotic transtibial prosthesis with biomechanical energy regeneration," *Ind. Robot*, vol. 36, no. 5, pp. 441–447, 2009.

[9] J. Zhu, Q. Wang, and L. Wang, "On the design of a powered transtibial prosthesis with stiffness adaptable ankle and toe joints," *IEEE Trans. Ind. Electron.*, vol. 61, no. 9, pp. 4797–4807, 2014.

[10] P. Cherelle, V. Grosu, A. Matthys, B. Vanderborght, and D. Lefeber, "Design and validation of the ankle mimicking prosthetic (AMP-) foot 2.0," *IEEE Trans. Neural Syst. Rehabil. Eng.*, vol. 22, no. 1, pp. 138–148, 2014.

[11] A. H. Shultz, J. E. Mitchell, D. Truex, B. E. Lawson, and M. Goldfarb, "Preliminary evaluation of a walking controller for a powered ankle prosthesis," in *Proc. Int. Conf. Robotics Automation*, 2013, pp. 4838–4843.

[12] (2014, Feb. 22). BiOM Personal Bionics. [Online]. Available: http://www.biom.com/

[13] SpringActive. (2014, Feb. 22). Providing innovative solutions to powered human assistance. [Online]. Available: http://www.springactive.com/

[14] E. H. Sinitski, A. H. Hansen, and J. M. Wilken, "Biomechanics of the ankle-foot system during stair ambulation: Implications for design of advanced ankle-foot prostheses," *J. Biomech.*, vol. 45, no. 3, pp. 588–594, 2012.

[15] L. Fradet, M. Alimusaj, F. Braatz, and S. I. Wolf, "Biomechanical analysis of ramp ambulation of transtibial amputees with an adaptive ankle foot system," *Gait Posture*, vol. 32, no. 2, pp. 191–198, 2010.

[16] (2014, Feb. 22). Proprio Foot. [Online]. Available: http://www.ossur.com/

[17] M. Palmer, "Sagittal plane characterization of normal human ankle functions across a range of walking gait speeds," M.S. thesis, Dept. Mech. Eng., Massachusetts Inst. Technol., Cambridge, MA, 2002.

[18] D. H. Gates, "Characterizing ankle function during stair ascent, descent, and level walking for ankle prosthesis and orthosis design," M.S. thesis, Dept. Biomed. Eng., Boston Univ., Boston, MA, 2004.

[19] F. Sup, A. Bohara, and M. Goldfarb, "Design and control of a powered transfemoral prosthesis," *Int. J. Robot. Res.*, vol. 27, no. 2, pp. 1–12, 2008.

[20] R. Riener, M. Rabuffetti, and C. Frigo, "Stair ascent and descent at different inclinations," *Gait Posture*, vol. 15, no. 1, pp. 32–44, 2002.

[21] A. S. McIntosh, K. T. Beatty, L. N. Dwan, and D. R. Vickers, "Gait dynamics on an inclined walkway," *J. Biomech.*, vol. 39, no. 13, pp. 2491–2502, 2006.

[22] C. Kendell, E. D. Lemaire, N. L. Dudek, and J. Kofman, "Indicators of dynamic stability in transtibial prosthesis users," *Gait Posture*, vol. 31, no. 3, pp. 375–379, 2010.

[23] J. L. Patton, Y. Pai, and W. A. Lee, "Evaluation of a model that determines the stability limits of dynamic balance," *Gait Posture*, vol. 9, no. 1, pp. 38–49, 1999.

Qining Wang, The Robotics Research Group, College of Engineering, Peking University, Beijing 100871, China. E-mail: qiningwang@pku.edu.cn.

Kebin Yuan, The Robotics Research Group, College of Engineering, Peking University, Beijing 100871, China. E-mail: kebin.yuan@pku.edu.cn.

Jinying Zhu, The Robotics Research Group, College of Engineering, Peking University, Beijing 100871, China. E-mail: jinyingzhu@pku.edu.cn.

Long Wang, The Robotics Research Group, College of Engineering, Peking University, Beijing 100871, China. E-mail: longwang@pku.edu.cn.